

Inertial Parameter Identification Including Friction and Motor Dynamics

Silvio Traversaro¹, Andrea Del Prete², Riccardo Muradore³, Lorenzo Natale² and Francesco Nori¹

Abstract—Identification of inertial parameters is fundamental for the implementation of torque-based control in humanoid robots. At the same time, good models of friction and actuator dynamics are critical for the low-level control of joint torques. We propose a novel method to identify inertial, friction and motor parameters in a single procedure. The identification exploits the measurements of the PWM of the DC motors and a 6-axis force/torque sensor mounted inside the kinematic chain. The partial least-square (PLS) method is used to perform the regression. We identified the inertial, friction and motor parameters of the right arm of the iCub humanoid robot. We verified that the identified model can accurately predict the force/torque sensor measurements and the motor voltages. Moreover, we compared the identified parameters against the CAD parameters, in the prediction of the force/torque sensor measurements. Finally, we showed that the estimated model can effectively detect external contacts, comparing it against a tactile-based contact detection. The presented approach offers some advantages with respect to other state-of-the-art methods, because of its completeness (i.e. it identifies inertial, friction and motor parameters) and simplicity (only one data collection, with no particular requirements).

I. INTRODUCTION

The relationship between joint torques and accelerations of a multi-body mechanical system is uniquely characterized by its inertial and geometric parameters. While geometric parameters can be accurately retrieved from CAD drawings, inertial parameters (i.e. masses, centers of mass, moments of inertia) typically need to be estimated. If we can effectively control the joint torques, inertial parameters are all we need to know to control the motion of a robot. However, controlling joint torques is usually difficult, especially because of the large joint friction that is a characteristic of gearboxes typically adopted in humanoid robots.

Different approaches to compensate for friction exist, but we can divide them in two big groups: feedback and feedforward. Feedback schemes exploit torque measurements to compensate for friction, often through the design of a friction observer [1] or a high-gain integral action [2]. Feedforward schemes, instead, use a previously identified friction model to predict friction, based on position, velocity and torque measurements [3]. Researchers proposed countless friction models [4] for control and simulation. In this paper

we consider a basic Coulomb and viscous friction model, because it captures most of the friction in our robot, while maintaining the estimation problem linear.

Dynamic parameter identification procedures are usually affected by problems such as identifiability of the considered parameters and numerical conditioning [5]. To solve this issues we used the Partial Least Square (PLS) regression method [20].

II. RELATED WORKS

To localize this work in the vast literature of robot dynamics identification we need to introduce the basic equations of robot and motor dynamics. The equation of motion of a multi-body system composed of n joints and n_B links can be written in a form that is linear with respect to the inertial parameters [5]:

$$Y_\tau(q, \dot{q}, \ddot{q})\phi = \tau,$$

where $\tau \in \mathbb{R}^n$ are the joint torques, $q \in \mathbb{R}^n$ are the joint angles, $Y_\tau(q, \dot{q}, \ddot{q}) \in \mathbb{R}^{n \times 10n_B}$ is the joint torque regressor matrix, and $\phi \in \mathbb{R}^{10n_B}$ contains the inertial parameters of all the links of the robot. Considering DC motors as actuators, the joint torques τ are given by the difference between the motor torques τ_m and the friction torques τ_F :

$$\tau = \underbrace{\Phi_m i}_{\tau_m} - \underbrace{Y_F(\dot{q})\phi_F}_{\tau_F}, \quad (1)$$

where $\Phi_m = \text{diag}(\phi_m) \in \mathbb{R}^{n \times n}$ contains the motor drive gains, $i \in \mathbb{R}^n$ are the motor currents, $\phi_F \in \mathbb{R}^{4n}$ contains four parameters for each joint describing asymmetric Coulomb and viscous frictions, and $Y_F(\dot{q}) \in \mathbb{R}^{n \times 4n}$ is the friction regressor matrix. The same model also applies if we can control the motor voltage v , rather than the current i . Neglecting the electrical dynamics (which is reasonable because the dynamics of the current amplifiers have much higher bandwidth than the motors) we have that:

$$i = \frac{1}{R}v + \underbrace{\frac{k_b}{R}\dot{q}}_{i_b}, \quad (2)$$

where i_b is proportional to the back electromotive torque and R is the motor coil resistance. If we substitute (2) in (1), the equation maintains the same form, because the back electromotive torque can be incorporated inside the viscous friction torque, being both terms proportional to \dot{q} . For this reason, in the following we do not make any distinction between voltage and current measurements.

Table I lists different works on robot dynamics identification (including the one presented here). We report which

*This paper was supported by the FP7 EU projects CoDyCo (No. 600716 ICT 2011.2.1 Cognitive Systems and Robotics (b)), Xperience(No. 270273), and ROBOSKIN (No. 231500).

¹Department of Robotics, Brains and Cognitive Sciences, Istituto Italiano di Tecnologia, Genova, Italy name.surname@iit.it

²Department iCub Facility, Istituto Italiano di Tecnologia, Genova, Italy name.surname@iit.it

³Department of Computer Science, University of Verona, Verona, Italy riccardo.muradore@univr.it

TABLE I

Author, Year	Knowns				Unknowns		
	v/i	τ	w	ϕ_m	ϕ_m	ϕ_F	ϕ
Atkeson, 1985 [6]	×			×			×
Iagnemma, 1998 [7]			×				×
Armstrong, 1988 [3]	×			×		×	×
Siciliano, 2009 [8]	×			×		×	×
Albu-Schaffer, 2001 [9]		×					×
	×	×			×	×	
Gautier, 2011 [10]	×				×	×	×
Chan, 2001 [11]	×		×		×		
	×			×		×	×
Traversaro, 2013	×		×		×	×	×

^{*} They attached a known load to the manipulator.

quantities are considered as *known*, either because measured — such as voltages v , currents i , joint torques τ , 6-axis forces/torques w — or because known constants — such as drive gains ϕ_m . Moreover we report which parameters are estimated (i.e. motor, friction and inertial parameters). The drive gains ϕ_m appear twice, because sometimes they are known, while other times they are estimated.

Atkeson et al. [6] used current measurements and drive gains ϕ_m to compute motor torques τ_m , and then to estimate the inertial parameters. They could neglect friction because their manipulator was direct drive, hence it had much less friction than the highly geared robots used in all other works. Iagnemma et al. [7] estimated the inertial parameters ϕ of a manipulator using a 6-axis F/T sensor mounted below the robot’s base. Armstrong [3] estimated motor torques τ_m from current measurements i and then he identified both inertial and friction parameters. The same approach is suggested in the well-known book by Siciliano and Sciavicco [8]. Albu-Schaffer and colleagues [9] estimated ϕ using joint torque sensors rather than a 6-axis F/T sensor. Moreover, they carried out a second identification to estimate motor dynamics and joint frictions. Gautier et al. [10] used only current measurements to estimate motor, friction and inertial parameters. In general this is possible only up to a proportional factor, because the equation to solve takes this form:

$$\begin{bmatrix} Y_\tau & -\text{diag}(i) & Y_F \end{bmatrix} \begin{bmatrix} \phi \\ \phi_m \\ \phi_F \end{bmatrix} = 0 \quad (3)$$

Gautier solved this issue by making the robot perform the same trajectories two times, one of which with a known load attached to its end-effector. Chan et al. [11] estimated first the motor parameters ϕ_m using current measurements and an external F/T sensor; then they identified ϕ and ϕ_F using i and the previously estimated ϕ_m . Our approach is similar to the work of Gautier [10], because we estimate all parameters at the same time as they did. However, rather than attaching a known load to the manipulator, we exploit a 6-axis F/T sensor mounted along the kinematic chain.

We now provide the reasons that led us to choose this estimation procedure. First, even if joint torque sensors and F/T sensors allow identifying inertial parameters only, we think it is paramount to identify friction parameters too. The final goal is to control the robot: if we do not identify

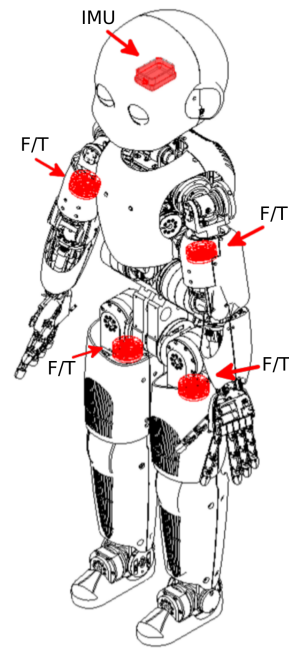


Fig. 1. **Top**: a mechanical scheme of the humanoid robot iCub: in evidence, the four proximal six-axis F/T sensors (legs and arms) and the inertial measurement unit (IMU) (head).

friction, the controller is going to have a hard time trying to compensate for it by using feedback only. Second, we think that it is important to identify also the drive gains ϕ_m , even if the motor manufacturers provide them, because there may be significant inaccuracies [10]. Moreover, the actual control signals are not the motor voltages v but the PWM signals, whose proportional relationship to v depends on the power supply voltage. Since the power supply voltage may change on different platforms (and even with time), this gives us another reason to identify ϕ_m .

III. PLATFORM

Experiments have been conducted on the iCub [12]. iCub is a full-body humanoid with 53 degrees of freedom: 6 in the head, 16 in each arm, 3 in the torso and 6 in each leg.

Numerical computations have been implemented relying on iDyn¹, a library for computing dynamics of kinematic trees. iDyn is built on top of iKin [13]², a library for forward-inverse kinematics of serial chains described in standard Denavit-Hartenberg notation. Both libraries are released under a GPL license.

As shown in Fig. 1, iCub is equipped with one inertial measurement unit (Xsens MTx-28A33G25³) located in the head and with four custom-made six-axis F/T sensors, one per limb, that are placed in the middle of the limbs, as shown in Fig. 1.

¹Doxygen documentation of the iDyn library available here: http://wiki.icub.org/iCub/main/dox/html/group__iDyn.html

²Doxygen documentation of the iKin library available here: http://wiki.icub.org/iCub/main/dox/html/group__iKin.html

³The MTx orientation tracker, <http://www.xsens.com/en/general/mtx>

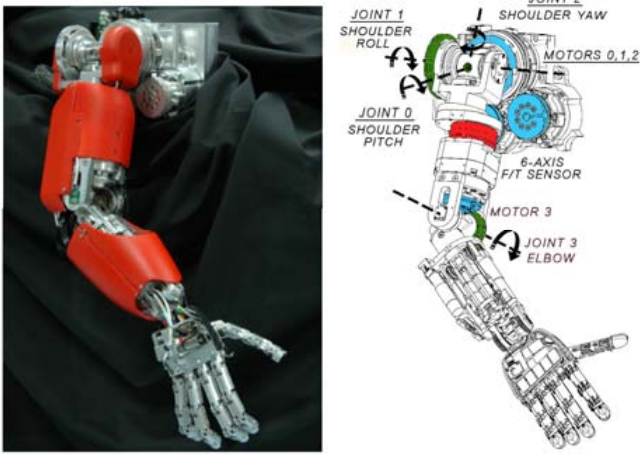


Fig. 2. A CAD view of the iCub arm showing its main DoFs, the location of the motors (blue) and the six-axis force/torque sensor (red).

The iCub upper body is covered with a distributed set of capacitive elements acting as tactile sensors [15], [16]. At the moment the iCub upper body is covered with approximately 2000 sensors. In this work we used these sensors to detect external contacts. The entire sensor network acts as an “artificial skin”, constituted by a sandwich of different flexible fabrics mounted on top of a flexible Printed Circuit Board (PCB), so that the entire structure can be conformed on surfaces of different curvatures. Fig. 3 shows the forearm with details on the distributed tactile sensor.

IV. METHOD

A. Regressor structure

The iCub arm is composed by 6 links. The third link contains the embedded F/T sensor, so for identification purposes it is convenient to consider separately the inertial contribution of its two sublinks. The inertial properties of a link are completely described by 10 parameters (mass, center of mass and inertia matrix) so the inertial parameters of the whole arm can be represented as a vector $\phi \in \mathbb{R}^{70}$ [5]. We now examine how inertial, friction and motor parameters are related to the available measurements (i.e. internal F/T sensor and PWM of the first four motors), under the assumption that no external forces act on the arm.

1) *F/T sensor dynamics*: each of the 6 components measured by the F/T sensor has an unknown offset, which can be represented by a 6 element vector w_O . We can write the dynamics of the F/T sensor as:

$$Y_s \phi + w_O = w_s, \quad (4)$$

where w_s is the measured wrench, and Y_s is the regressor of inertial and gravitational wrench.

2) *Elbow joint*: the elbow (joint 3) of the arm of the iCub is actuated by a dedicated motor, so we can directly write the dynamics of the joint as:

$$\phi_{m_3} v_3 = Y_{\tau_3} \phi + Y_{F_3} \phi_{F_3}, \quad (5)$$

where:

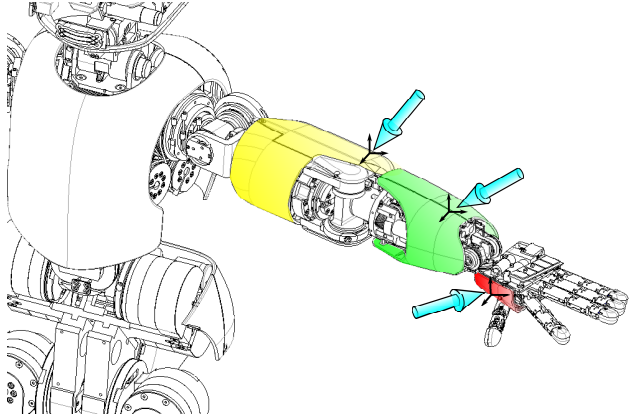
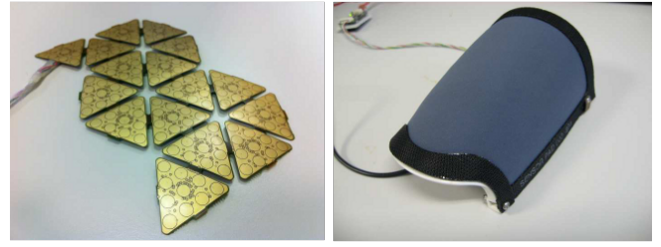


Fig. 3. **Top**: the iCub forearm with the distributed tactile elements. The left picture shows the flexible PCB to be mounted on the forearm; the right picture shows the assembly with the capacitive element mounted on top of the lower forearm cover. Details about skin fabrication and the covering of the iCub can be found in the Roboskin website, EU Project ICT-FP7-231500 Roboskin. **Bottom**: a visualization of the iCub right arm which has been used in the experiments presented in this paper; the picture highlights with colors the sensorized areas.

ϕ_{m_k} is the constant relating the PWM of the motor k to the exerted torque

v_k is the PWM of the motor k

Y_{τ_j} is the regressor of inertial and gravitational torques for joint j

ϕ_{F_j} is the vector of asymmetric Coulomb and viscous friction coefficients $[\phi_j^{c+} \ \phi_j^{c-} \ \phi_j^{v+} \ \phi_j^{v-}]^\top$

Y_{F_j} is the regressor of friction torques $[(\text{sgn } \dot{q}_j)^+ \ -(\text{sgn } \dot{q}_j)^- \ (\dot{q}_j)^+ \ -(\dot{q}_j)^-]$

The operators $()^+$ and $()^-$ select the positive and negative part (respectively) of the argument. There is no distinction between the friction acting on the joint and on the motor, because the joint is actuated by a dedicated motor. We can rewrite (5) as linear with respect to the unknown parameters:

$$[Y_{\tau_3} \ Y_{F_3} \ -v_3] \begin{bmatrix} \phi \\ \phi_{F_3} \\ \phi_{m_3} \end{bmatrix} = 0 \quad (6)$$

3) *Shoulder joints*: the shoulder group is composed of the joints 0, 1 and 2. We refer to this group as I , defining $q_I^\top = [q_0 \ q_1 \ q_2]$ and $\tau_I^\top = [\tau_0 \ \tau_1 \ \tau_2]$. The dynamics of the shoulder joints are:

$$\tau_I = Y_{\tau_I} \phi + Y_{F_I} \phi_{F_I}, \quad Y_{F_I} = \begin{bmatrix} Y_{F_0} & 0 & 0 \\ 0 & Y_{F_1} & 0 \\ 0 & 0 & Y_{F_2} \end{bmatrix}, \quad (7)$$

where:

$$\phi_{F_I}^\top = [\phi_0^{c+} \phi_0^{c-} \phi_0^{v+} \phi_0^{v-} \phi_1^{c+} \phi_1^{c-} \phi_1^{v+} \phi_1^{v-} \phi_2^{c+} \phi_2^{c-} \phi_2^{v+} \phi_2^{v-}]^\top$$

These friction coefficients are related to the joint frictions, which in this case must be distinguished from the motor frictions, because of the coupling. The relationship between the motor torques and the joint torques is given by:

$$\tau_I = T^\top \tau_{m_I}, \quad T^\top = \begin{bmatrix} 1 & -r & -r \\ 0 & r & r \\ 0 & 0 & r \end{bmatrix}, \quad (8)$$

where T is the coupling matrix, with $r = \frac{65}{40} = 1.625$. For further details on the shoulder coupling see [18]. The relationship between the motor torques and the motor voltages is:

$$\tau_{m_I} = \text{diag}(\phi_{m_I}) v_I - Y_{F_I^m} \phi_{F_I^m}, \quad (9)$$

where $Y_{F_I^m}$ is similar to the regressor Y_{F_I} , but with the motor velocities $\dot{q}_{m_I}^\top = [\dot{q}_{m_0} \dot{q}_{m_1} \dot{q}_{m_2}]$ in place of the joint velocities \dot{q}_I . Substituting (8) and (9) into (7) we can write an equation that is linear with respect to all the parameters:

$$\begin{bmatrix} Y_{\tau_I} & Y_{F_I} & T^\top Y_{F_I^m} & -T^\top \text{diag}(v_I) \end{bmatrix} \begin{bmatrix} \phi \\ \phi_{F_I} \\ \phi_{F_I^m} \\ \phi_{m_I} \end{bmatrix} = 0 \quad (10)$$

4) *Complete regressor*: by combining all the parameters in a unique vector, we can write (4), (6) and (10) in a unified matrix equation:

$$\begin{bmatrix} Y_{\tau_I} & 0 & Y_{F_I} & 0 & T^\top Y_{F_I^m} & -T^\top \text{diag}(v_I) & 0 \\ Y_{\tau_3} & 0 & 0 & Y_{F_3} & 0 & 0 & -v_3 \\ Y_{F_T} & I_{6 \times 6} & 0 & 0 & 0 & 0 & 0 \end{bmatrix} \begin{bmatrix} \phi \\ w_O \\ \phi_{F_I} \\ \phi_{F_3} \\ \phi_{F_I^m} \\ \phi_{m_I} \\ \phi_{m_3} \end{bmatrix} = \begin{bmatrix} 0 \\ 0 \\ w_s \end{bmatrix} \quad (11)$$

As opposed to (3) this is a non-homogeneous equation, which allows us to avoid the ‘‘proportional factor’’ problem. However, not all the inertial parameters can be identified, because of the structural properties of the regressors Y_τ and Y_{F_T} [5]. The regression method introduced in the next section allows us to readily solve this issue.

B. Partial Least Squares (PLS)

At time t equation (11) can be rewritten in a compact form as:

$$Y_{ALL}(t)\Phi = w_{ALL}(t) \quad (12)$$

The identification procedure is based on time series for the matrix $Y_{ALL}(t)$ and the vector $w_{ALL}(t)$: collecting the input-output data in the matrix A and the vector b , we end up with the linear equation:

$$A\Phi = b + e, \quad (13)$$

where e is the vector taking into account the measurement error and the unmodeled dynamics, and Φ is the unknown vector we need to estimate.

Following [19], we use the Partial Least Square (PLS) method to solve (13). This technique is very popular in chemometrics and statistical process control because it is extremely stable even with highly collinear data. The PLS goal is twofold: to explain the variance of the input matrix A (as the principal component analysis, PCA, does) and to maximize the covariance between A and the output vector b . The nonlinear iterative partial least squares (NIPALS, [20]) computes the so-called score-loading decomposition of A and b as:

$$A = \sum_{i=1}^{\nu} t_i p_i^\top + E_A = TP^\top + E_A \quad (14)$$

$$b = \sum_{i=1}^{\nu} t_i c_i^\top + e_b = TC^\top + e_b, \quad (15)$$

where ν is the number of latent variables, t_i are the common scores, p_i and c_i are the A - and b -loadings, respectively. In [21], the structural properties of these matrices are stated. In the present case the value of ν is strictly related to the number of base parameters.

The estimation of Φ is:

$$\hat{\Phi} = W(P^\top W)^{-1}C, \quad (16)$$

where $W = [w_1 \ w_2 \ \dots \ w_\nu]$ and the vectors w_k are computed in the PLS algorithm as a side-product of the score-loading decomposition. The matrix W is related to A by $T = AW(P^\top W)^{-1}$, where the matrix $P^\top W$ is nonsingular by construction.

C. Anomaly detection

In process control, many indices have been developed to check if the system is *statistically* in- or out-of-control, mainly for safety reason (fault detection and isolation, FDI). See also [22] for a robotic application. Among the available indices, the Hotelling or T^2 statistics is defined as:

$$T^2(t) \triangleq e^\top(t)\Lambda_e^{-1}e(t), \quad \Lambda_e = \text{diag}\{\sigma_1^2, \dots, \sigma_n^2\}, \quad (17)$$

where $e = y - \hat{y}$ is the error, and the variances $\sigma_i^2 = \text{Var}\{e_i(\cdot)\}$ are computed during the identification phase. The plant is statistically in-control if $T^2(t) \leq T_\alpha^2$. Under the assumption of normally distributed data, the upper bound T_α^2 with confidence level α is given by:

$$T_\alpha^2 \triangleq \frac{n(N-1)}{(N-n)} F_{n, N-n; \alpha}, \quad (18)$$

where n is the number of LVs (ν in our case), N is the number of samples in the calibration data and F is the Snedecor (or F) distribution with degrees of freedom n and $N-n$, [23]. The threshold (18) is only an approximation because our data is not following exactly a normal distribution and our model is an approximation of the real plant.

In this work we use the estimated and validated inertial parameters to compute T^2 statistics on new data, for detecting when the robot gets in contact with the environment. In other words, the ‘‘fault’’ in the present case is the contact that ‘‘invalidates’’ the estimation using $\hat{\Phi}$.

V. RESULTS

We tested the proposed identification scheme on the right arm of the iCub. We carried out two experiments of 5 minutes each, using impedance control to make the right hand reach pseudo-random points in the Cartesian space, without making contact with anything. During the tests, we collected joint angle, 6-axis force/torque and PWM measurements. Joint velocities and accelerations were estimated offline using a noncausal adaptive window technique [24]. We used the first dataset to identify the model parameters and the second dataset to validate the identified model.

The result of the validation are presented in Fig. 4, which shows the validation errors using the T^2 index. On all the samples of the validation dataset, except for a few outliers, the prediction of the dynamics (using the parameters estimated on the first dataset) is lower than the confidence threshold T_α^2 (with a confidence level of $\alpha = 0.99$).

To further validate our model, we compared the prediction errors obtained using the parameters extracted from the 3D mechanical drawings (CAD, Computer Aided Manufacturing)⁴ with those estimated using PLS. As the motor voltage measurements depend also on motor gains and friction coefficients, it is not possible to predict them using the CAD parameters, so, for this validation, only the prediction of the F/T sensor was used. We measured a remarkable improvement in the force prediction, whereas the torque prediction error is approximately the same (see Table II).

TABLE II
FORCE/TORQUE SENSOR PREDICTION ERRORS.

	Estimated parameters		CAD parameters	
	<i>mean</i>	<i>std dev</i>	<i>mean</i>	<i>std dev</i>
\mathbf{F} (N)	1.33	0.64	1.86	0.59
$\boldsymbol{\tau}$ (Nm)	0.15	0.13	0.15	0.07

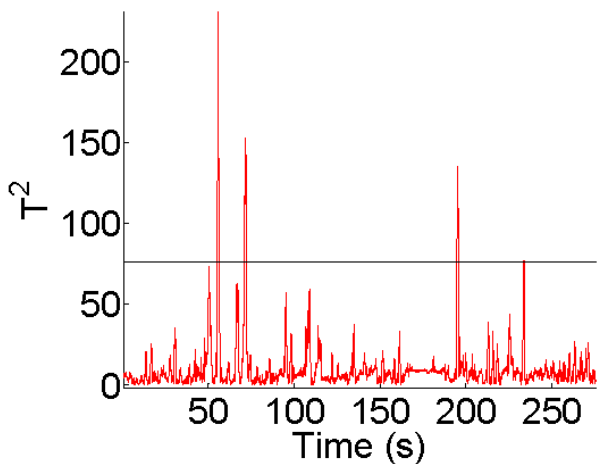


Fig. 4. T^2 index during the validation trajectory without external contacts. The horizontal line indicates the T_α^2 threshold (with $\alpha = 0.99$).

⁴CAD models and drawings of the iCub are available under an open source license: <http://wiki.icub.org/wiki/RobotCub>

Next, we used the identified model to detect external contacts. We carried out another experiment, similar to the previous one, but with the difference that, from time to time, we touched the iCub's arm on its tactile sensors. Besides the measurements of the previous test, we also collected the tactile sensor measurements, to use them as ground truth for the contact detection. To detect contacts we monitored the T^2 index: when it exceeds the T_α^2 threshold (with $\alpha = 0.99$), we infer that an external force is perturbing the system dynamics. Fig. 5 shows part of the results. Using

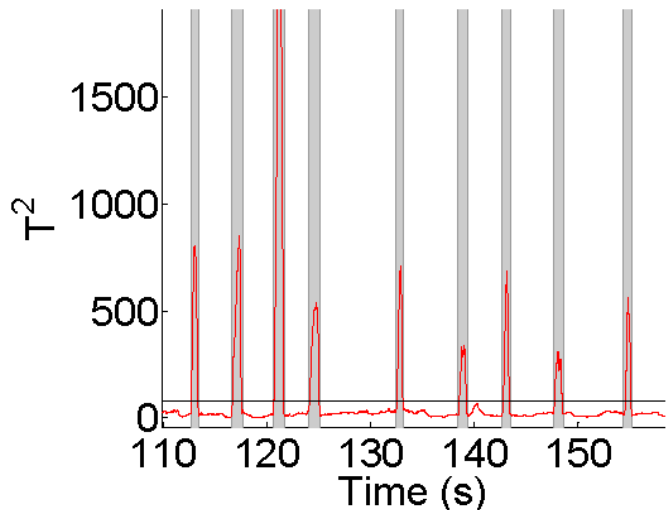


Fig. 5. T^2 index during the test with external contacts. The grey areas correspond to the periods of time when the tactile sensors were detecting contact. When the T_α^2 threshold (the horizontal line) is exceeded we infer that an external force is perturbing the system dynamics.

this threshold we obtain a true positive rate (i.e. ratio between true and actual positives) of 67% and a false positive rate (i.e. ratio between false positives and actual negatives) of 6%. Fig. 6 shows how the two rates (true positive and

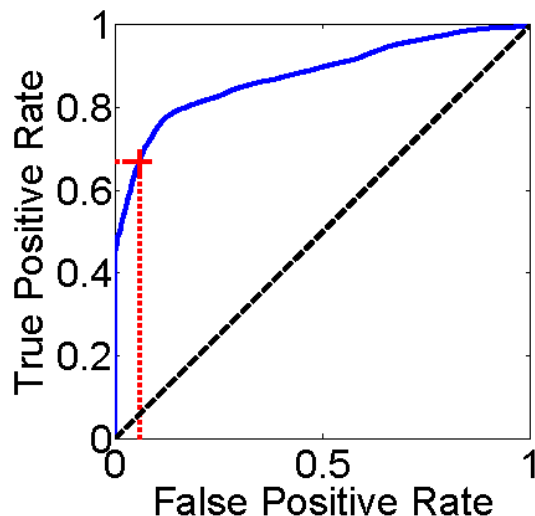


Fig. 6. Receiver Operating Characteristic curve for contact detection. The cross indicates the point corresponding to the T_α^2 threshold, with $\alpha = 0.99$.

false positive) change in our experiment by varying the T^2

threshold.

VI. CONCLUSIONS AND FUTURE WORK

In this paper we propose a new identification scheme for estimating, in a unique procedure, the inertial, friction and motor parameters of a rigid robot actuated by DC motors. The identification exploits the measurements of the motor PWM and of an internal 6-axis force/torque sensor. To overcome the problem of the singularity of the regressor matrix, we used the PLS regression method, which is stable also with highly collinear data. We identified the dynamics of the right arm of the iCub robot and we verified that, in absence of external contacts, the identified model was able to accurately predict the force/torque sensor measurements. We also proved that the error between the force/torque sensor measurement and its model-based prediction can be monitored to detect external forces. In the experiments we used the tactile sensors of the iCub as ground truth for the contact detection task. The key points of the presented approach are:

- it estimates all the parameters that are necessary for implementing model-based controllers (e.g. computed torque control [8])
- it does not split the identification into subparts, so only one data collection has to be carried out [9]
- there is no need to attach known loads to the robot [10]
- it is applicable to any robot having a base force/torque sensor and current/voltage measurements

We plan to use the identified parameters for implementing a model-based control architecture. In particular, the motor and friction parameters will be used by the low-level controllers to implement joint torque control. Inertial parameters instead will be used for computing the inverse dynamics of the robot.

Inertial parameters are time-invariant, and they cannot be estimated when the robot makes contact. On the other hand, friction and motor parameters may change with time, so we intend to design an online estimation scheme, which can work even in presence of external contacts. Moreover, the estimation of the drive gains would benefit from external forces; this is because, in absence of contacts, the motor torques are usually small (especially when accelerating light-weight links, such as the iCub's forearm), making the estimation of the drive gains ill-conditioned.

REFERENCES

- [1] L. L. Tien and A. Albu-Schäffer, "Friction Observer and Compensation for Control of Robots with Joint Torque Measurement," in *Intelligent Robots and Systems, IROS. IEEE/RSJ International Conference on*, 2008, pp. 22–26.
- [2] G. Morel, K. Iagnemma, and S. Dubowsky, "The precise control of manipulators with high joint-friction using base force/torque sensing," *Automatica*, vol. 36, no. 36, pp. 931–941, 2000.
- [3] B. S. R. Armstrong, "Dynamics for Robot Control: Friction Modeling and Ensuring Excitation During Parameter Identification," Ph.D. dissertation, Stanford University, 1988.
- [4] H. Olsson, K. J. Åström, C. Canudas de Wit, M. Gäfvert, and P. Lischinsky, "Friction models and friction compensation," *European journal of control*, vol. 4, pp. 176–195, 1998.
- [5] J. Hollerbach, W. Khalil, and M. Gautier, "Model Identification," in *Springer Handbook of Robotics*, B. Siciliano and O. Khatib, Eds. Springer Berlin Heidelberg, 2008, pp. 321–344.
- [6] C. H. An, C. G. Atkeson, and J. M. Hollerbach, "Estimation of inertial parameters of rigid body links of manipulators," in *Decision and Control, 1985 24th IEEE Conference on*, vol. 24. IEEE, 1985, pp. 990–995.
- [7] G. Liu, K. Iagnemma, S. Dubowsky, and G. Morel, "A base force/torque sensor approach to robot manipulator inertial parameter estimation," *Robotics and Automation, IEEE International Conference on*, vol. 4, no. May, pp. 3316–3321, 1998.
- [8] B. Siciliano and L. Sciacivico, *Robotics: modelling, planning and control*. Springer, 2009.
- [9] A. Albu-Schäffer and G. Hirzinger, "Parameter identification and passivity based joint control for a 7 DOF torque controlled light weight robot," in *Robotics and Automation, 2001. Proceedings. ICRA'01. IEEE International Conference on*, 2001, pp. 2852–2858.
- [10] M. Gautier and S. Briot, "New Method for Global Identification of the Joint Drive Gains of Robots using a Known Payload Mass," in *Intelligent Robots and Systems, IEEE/RSJ International Conference on*, 2011, pp. 3728–3733.
- [11] S. Chan, "An efficient algorithm for identification of robot parameters including drive characteristics," *Journal of Intelligent and Robotic Systems*, pp. 291–305, 2001.
- [12] G. Metta, L. Natale, F. Nori, G. Sandini, D. Vernon, L. Fadiga, C. Von Hofsten, K. Rosander, M. Lopes, J. Santos-Victor, A. Bernardino, and L. Montesano, "The iCub humanoid robot: an open-systems platform for research in cognitive development." *Neural Networks*, vol. 23, no. 8-9, pp. 1125–1134, 2010.
- [13] U. Pattacini, F. Nori, L. Natale, G. Metta, and G. Sandini, "An experimental evaluation of a novel minimum-jerk cartesian controller for humanoid robots," in *Intelligent Robots and Systems (IROS), 2010 IEEE/RSJ International Conference on*. IEEE, 2010, pp. 1668–1674.
- [14] M. Fumagalli, S. Ivaldi, M. Randazzo, L. Natale, G. Metta, G. Sandini, and F. Nori, "Force feedback exploiting tactile and proximal force/torque sensing. Theory and implementation on the humanoid robot iCub," *Autonomous Robots*, vol. 33, no. 4, pp. 381–398, 2012.
- [15] G. Cannata, M. Maggiali, G. Metta, and G. Sandini, "An embedded artificial skin for humanoid robots," *2008 IEEE International Conference on Multisensor Fusion and Integration for Intelligent Systems*, pp. 434–438, 2008.
- [16] P. Maiolino, M. Maggiali, G. Cannata, G. Metta, and L. Natale, "A Flexible and Robust Large Scale Capacitive Tactile Sensor for Robots," *IEEE Sensors Journal*, 2013.
- [17] P. Fitzpatrick, G. Metta, and L. Natale, "Towards long-lived robot genes," *Robotics and Autonomous Systems*, vol. 56, no. 1, pp. 29–45, 2008.
- [18] A. Parmiggiani, M. Randazzo, L. Natale, G. Metta, and G. Sandini, "Joint torque sensing for the upper-body of the iCub humanoid robot," in *2009 9th IEEE-RAS International Conference on Humanoid Robots*. Ieee, Dec. 2009, pp. 15–20.
- [19] R. Muradore, R. Foroncelli, and P. Fiorini, "Statistical methods for estimating the dynamical parameters of manipulators," in *Decision and Control, 2009 held jointly with the 2009 28th Chinese Control Conference. CDC/CCC 2009. Proceedings of the 48th IEEE Conference on*. IEEE, 2009, pp. 6472–6477.
- [20] P. Geladi and B. R. Kowalski, "Partial least-squares regression: a tutorial," *Analytica chimica acta*, vol. 185, pp. 1–17, 1986.
- [21] I. S. Helland, "On the structure of partial least squares regression," *Communications in statistics-Simulation and Computation*, vol. 17, no. 2, pp. 581–607, 1988.
- [22] R. Muradore and P. Fiorini, "A PLS-Based Statistical Approach for Fault Detection and Isolation of Robotic Manipulators," *Industrial Electronics, IEEE Transactions on*, vol. 59, no. 8, pp. 3167–3175, 2012.
- [23] S. Joe Qin, "Statistical process monitoring: basics and beyond," *Journal of Chemometrics*, vol. 17, no. 8-9, pp. 480–502, 2003.
- [24] F. Janabi-Sharifi, "Discrete-time adaptive windowing for velocity estimation," *Control System Technology, IEEE Transactions on*, vol. 8, no. 6, pp. 1003–1009, 2000.